

IDENTIFICATION OF FGFR INHIBITOR AS ST2 RECEPTOR/INTERLEUKIN-1 RECEPTOR-LIKE 1 INHIBITOR IN CHRONIC OBSTRUCTIVE PULMONARY DISEASE DUE TO EXPOSURE TO E-CIGARETTES BY NETWORK PHARMACOLOGY AND MOLECULAR DOCKING PREDICTION

MUTHIA NURHIDAYAH¹, FADILAH FADILAH² , ADE ARSIANTI² , ANTON BAHTIAR¹ 

¹Department of Pharmacology, Faculty of Pharmacy, Universitas Indonesia, Gedung Fakultas Farmasi Kampus UI Depok 16424, Indonesia,

²Department of Medicinal Chemistry, Faculty of Medicine, Universitas Indonesia, Jl. Salemba Raya no 6, Indonesia

Email: anton.bahtiar@ui.ac.id

Received: 07 Dec 2021, Revised and Accepted: 10 Jan 2022

ABSTRACT

Objective: This study was designed to search for candidate drugs that act on IL-33 and ST2, which was carried out using a bioinformatics approach.

Methods: We first analyzed Network Electronic Cigarette Smokes Predictions of therapeutic targets by Cytoscape. We collected from the Swiss TargetPrediction database [http://www.swisstargetprediction.ch/] by inputting each compound structure of the electronic cigarette smoke in SDF format. The target protein data is then supplemented with UniProt ID data to uniform protein identity. We then identified COPD Related Targets in Humans by Cytoscape. Subsequently, we identified key receptors in the pathogenesis of COPD. All target proteins that have a significant role in the pathogenesis of COPD exposed to cigarette smoke will be known from the combination of this network.

Results: Based on the validation results of the protein receptor for ST2, a protein is used as a receptor with PDB ID: 1IRA. After analyzed by PyMol software, a protein with PDB ID 1IRA it has no missing residue in its sequence. Drug candidates analyzed by the structural similarity with the native ligand using PubChem and DRUGBANK analysis are follow: N-acetylmannosamine, Aceneuramic acid, Ceramide AP, Ceramide NP, Hg9a-9, Nonanoyl-N-hydroxyethylglucamide, N-Acetyl-2-deoxy-2-amino-galactose, N-Acetyllactosamine, MLI/2,6-dimethyl-4-[6-[5-[1-methylcyclopropyl]oxy-1H-indazol-3-yl] pyrimidin-4-yl] morpholine, Terazosin, BMS-911543, NAG Inhibitor, FGFR Inhibitor/sodium; 2-amino-5-[1-methoxy-2-methylindolizine-3-carbonyl] benzoate. After docking, the smallest or more negative binding affinity values are obtained. The stronger the FGFR Inhibitor ligand showed the interaction with the Receptor with a binding affinity value of -9.0 kcal/mol with mode/position 0, and RMSD 0.0. The second smallest binding affinity value is the NAG ligand with -8.5 kcal/mol with mode/position 0 and RMSD 0.0.

Conclusion: The findings revealed that FGFR Inhibitor was a suitable repurposing medication for anti-COPD development via the IL-33/ST-2 signaling pathway.

Keywords: COPD, ST2 Receptor, Interleukin-1 receptor-like 1, Network pharmacology, Molecular docking

© 2022 The Authors. Published by Innovare Academic Sciences Pvt Ltd. This is an open-access article under the CC BY license (<https://creativecommons.org/licenses/by/4.0/>)
DOI: <https://dx.doi.org/10.22159/ijap.2022v14i2.43784>. Journal homepage: <https://innovareacademics.in/journals/index.php/ijap>

INTRODUCTION

Electronic cigarettes or e-cigarettes are often advertised as a safe alternative way to help someone quit smoking. The number of electronic cigarette [vapers] users continues to increase in many countries. Many young people are now using these devices only for social aspects and only as a trend [1]. Although e-cigarettes are marketed as smoking cessation tools by some manufacturers, the reality is that many nonsmokers, including teenagers, use them [2].

A person with Chronic obstructive pulmonary disease or COPD struggling to quit smoking may consider using e-cigarettes as an alternative to smoking cessation. Some patients with COPD may have switched to dual-use or e-cigarette use only. The National Academies of Sciences, 2018 concluded that there are unclear results regarding whether the use of e-cigarettes in patients with COPD will be beneficial, neutral, or even harmful. Recent studies have not further explained whether switching to e-cigarettes from traditional tobacco cigarettes will reduce lung inflammation or disease progression in these patients. Traditional nicotine replacement therapy [NRT/Nicotine Replacement Therapy] is currently the safest choice for COPD patients because research has shown that e-cigarettes regulate inflammation and have adverse effects on the airways of e-cigarette users [3] and thus the negative impact on COPD patients cannot be avoided.

The pathogenesis of COPD includes oxidative stress, protease-antiprotease imbalance, and inflammation [4, 5]. Lipopolysaccharides [LPS] and cigarette smoke have been stimuli used in COPD research [6]. Cigarette smoke increases the production of reactive oxygen species [ROS]. It adds many pro-inflammatory cytokines such as IL-6 and IL-8 [7], and the lipid peroxidation

product malondialdehyde [MDA] is the most frequently measured indicator of oxidative damage in membrane lipids [8]. It is believed that there is a need for new therapies for candidates that exhibit antioxidant and anti-inflammatory properties for COPD.

The American Thoracic Society and other leading pulmonary disease organizations recommend that COPD patients quit smoking using one or more inhaled bronchodilators. Long-acting 2-adrenergic receptor agonists [LABA] and long-acting muscarinic acetylcholine receptor antagonists [LAMA] have additive effects on bronchodilation. At the same time, they produce effective bronchodilation but are less effective at treating the underlying inflammatory disease in patients with COPD [9]. Although glucocorticoids are the mainstay of therapy for COPD, it has been recognized that glucocorticoids do not work well in certain patient populations, which has been associated with decreased sensitivity [10]. Broad-spectrum anti-inflammatory drugs and pro-inflammatory enzyme inhibitors such as PDE-4 may be more effective, but there are side effects after oral administration, which is a major drawback [11]. Selective phosphodiesterase 4 [PDE-4] inhibitors have been shown to reduce airway inflammation and bronchoconstriction associated with COPD [12-15].

New molecularly targeted medications are being developed. Many new molecular targeted medications have been developed in recent years based on the molecular mechanism of COPD. Antioxidants minimize cellular damage and inflammation by scavenging ROS and inhibiting oxidative stress in the lungs. By inhibiting proteases, protease inhibitors restore the balance between protease and anti-protease. Inhibitors of cytokines and chemokines are important in lowering the inflammatory response. Adhesion molecule inhibitors can stop inflammatory cells that move from blood arteries to tissue.

PDE4 inhibitors work by preventing PDE4 from being produced and so increasing cAMP activity in cells. Signaling molecules like NF- κ B, MAPK, PI3K, and VIP regulate inflammation and airway remodelings during the onset and progression of COPD, and they could be used to develop treatment possibilities. Inhibitors of p38MAPK, NF- κ B, and PI3K, as well as a vasoactive intestinal peptide, are among the candidates [VIP]. The EGFR inhibitor lowers EGFR internalization but does not reduce mucin storage. Endothelin inhibitors limit the evolution of pulmonary hypertension in COPD patients by reducing fibrotic airway remodeling and downregulating MMP expression. Neutrophil superoxide generation, phagocytosis, adhesion, and cytokine release are all inhibited by the adenosine A2a receptor. Macrolides diminish COPD inflammation by inhibiting the generation of inflammatory cytokines via regulating the PI3K/Akt-Nrf2 pathway and controlling transcription factors such as NF- κ B and AP-1. By inhibiting NF- κ B and other pro-inflammatory transcription factors, PPAR agonists have antioxidant and anti-inflammatory effects [16].

Interleukin-33 is abundant in lung tissue and has a critical function in respiratory illness, which can induce airway inflammation, airway hyperresponsiveness, and goblet cell metaplasia in allergen-induced mice, and may exacerbate asthma-like responses in allergen-exposed mice. However, whether cigarette smoke can induce IL-33/ST2 expression in the airways and whether the IL-33 system contributes to the pathogenesis of cigarette smoke-mediated COPD is not known with certainty [17].

Several investigators reported that IL-33 and ST-2 could be induced in rats exposed to e-cigarette smoke; IL-33/ST-2 binding can trigger airway inflammation and mucin expression in the airways. Therefore, IL-33/ST-2 may be a new therapeutic target for respiratory disease mediated. CS includes COPD [18].

This study was designed to search for candidate drugs that act on IL-33/ST-2, which was carried out using a bioinformatics approach.

MATERIALS AND METHODS

Methods

The hardware used is a notebook with 11th Gen Intel[R] Core[™] i7-1165G7 @ 2.80GHz 2.80 GHz Installed RAM 16,0 GB, Edition Windows 11 Home Single Language

Version, 64-bit operating system, x64-based processor. The software used is PyRx [Vina and AutoDock], MarvinBean Suite, PyMOL, PLIP, Chimera, and Discovery Studio 2021.

Molecular targeting

Collecting a chemical structure database of e-cigarette content compounds

At this stage, information on the chemical content of e-cigarettes will be collected both from the results of previous publications and from available databases. Furthermore, the chemical structure was obtained from PubChem [<https://pubchem.ncbi.nlm.nih.gov/>] and then saved in SDF format for further prediction phase therapeutic targets.

Prediction of therapeutic targets of electronic cigarette content on receptors that play a role in COPD pathogenesis

Predictions of therapeutic targets were collected from the Swiss Target Prediction database [<http://www.swisstargetprediction.ch/>] by inputting each compound's Structure in SDF format. The target protein data is then supplemented with UniProt ID data to uniform protein identity. Then the target protein data for the compounds contained in the electronic cigarette was then compiled in excel format and analyzed using Cytoscape.

Creation of a database of receptors involved in COPD pathogenesis

The Database was created based on the Disgenet, Uniprot, Therapeutic Target Database [TTD], and DrugBank websites. Data was completed with Uniprot ID to uniform protein identity. All protein targets obtained were compiled in excel format. The data were then analyzed using Cytoscape software to identify proteins that have a significant role in the

pathogenesis of COPD. Network analysis was performed to determine the degree and betweenness centrality of each protein node using Cytoscape software. The significance level of protein on the pathogenesis of COPD was measured based on the degree value. The higher the degree value indicates, the greater the significance of a node in the network, or at this stage, it means the greater the protein significance in COPD pathogenesis.

Identification of key receptors for COPD pathogenesis targeted by compounds contained in e-cigarettes

At this stage, merging is carried out between two networks, namely the COPD pathogenesis network and the protein target network of compounds contained in electronic cigarettes. From the combination of this network, all target proteins that have a significant role in the pathogenesis of COPD will be known. These proteins were then collected for their three-dimensional protein structure on the PDB website [<https://www.rcsb.org/>]. The three-dimensional protein structure is stored in PDB format for use in the molecular docking stage.

Selection of drug compounds based on pharmacophore mapping

Structure and ligand-based pharmacophore modeling

ST2 antagonists are obtained by collecting all available target annotations from ChEMBL. To generate a structure and ligand-based pharmacophore model, ST2 antagonists were obtained from ChEMBL [<https://www.ebi.ac.uk/chembl/>]. A literature search was carried out with ST2 annotations [PDB ID: 1IRA] then docking analysis was performed to determine binding affinity value. The best compound with the lowest binding affinity [kcal/mol] was selected for structure and ligand-based pharmacophore modeling. LigandScout 4.3 software was used to generate a structure and ligand-based pharmacophore model in the next process.

Pharmacophore model validation

At this stage, an evaluation of the potential description of the active and inactive compounds obtained from certain protein-ligand interactions is carried out. The pharmacophore model generated from the protein-ligand complex was validated for its performance to discriminate the active compound by screening some known active compounds in the first step and decoy obtained from the DUD-E database. The Database of DUD-E was converted in. ldb format before being filtered using the "create screening database" menu of LigandScout 4.3. then see the value of the quality of the structure-based model based on the ROC curve with the AUC score and enrichment factor [EF].

Generalized dataset for basic pharmacophore screening

At this stage, new and active molecules were identified by performing virtual screening in the previously generated pharmacophore model. The ZINC database [<https://zinc.docking.org/>] was used to identify compounds that have potential against protein targets. In selecting candidate compounds, it is preferred to choose compounds that have the most similar features to the required pharmacophore features so that they can easily interact with the target protein. Then the possible hit compound, which has its maximum features matched the pharmacophore, is selected.

Pharmacophore based virtual screening

At this stage, the Database generated from ZINC was filtered against the validated structural-based pharmacophore features. LigandScout 4.3 was used to create and obtain 3D models of protein-ligand interactions and convert compounds into a file format [IDB]. These compounds are passed directly to the list database for rapid virtual screening based on pharmacophore features. The hit compound used was compiled based on the pharmacophore fit score and used for further validation.

Screening of substance protein targets in E-cigarettes related to conditions that cause COPD

Electronic cigarette compound collection

Information on the content of each puff of e-cigarettes is obtained from the research conducted by Cunningham *et al.*, 2020 [19].

Each of the above compounds collected target protein data both from databases such as PubChem, SwissADME and SwissPrediction, PharmMapper, can also be retrieved from GeneCards V4.12 [https://www.genecards.org/] and OMIM [https://omim.org/] [20-23].

COPD related targets in humans

Cytoscape installed using STRING databases can be used to create COPD target networks. Using the keyword "chronic obstructive pulmonary disease," we got networking in the form of nodes related to COPD in humans [24].

Target screening

The target set in point [a] is networked using Cytoscape, and then a target slice is made using COPD networking [b].

Using cytoNCA installed in Cytoscape, the network containing the above targets will be analyzed: degree, eigenvector centrality, LAC centrality, closeness centrality, network centrality of all nodes. The average value of the analysis results is used as a standard for target selection. The Protein-protein Interaction [PPI] Network is obtained from considering the existing nodes as the main node [25].

Protein-protein interaction analysis

Using the STRING database, the results are more likely to point to protease inhibitors-neutrophils, but if the <http://www.interactome-atlas.org/search#> gene analysis shows the best value when set to the confidence level, to identify gene that plays an essential role in the main target of compounds against COPD [26, 27].

Search and evaluate ST2 or IL1RL1 protein from the database as a target receptor

Proteins for analysis in this study were obtained from the RCSB database with IL33 or ST2 or the synonym IL1RL1. To determine whether the protein can be used well in docking, it is evaluated first in 3 ways. The first is by directly analyzing the protein data in the RCSB database [such as resolution values<3, wwPDB Validation percentile ranks, and ligand structure quality assessment] [28, 29]. The second is to access PDBSUM using the Ramachandran plot to evaluate the most favored value of at least 90% and the G factor [30], And the third is to analyze the missing residue using PyMol [31].

Collection of ligands/ drug candidates from the PubChem database

The initial stage is to search for drug candidates by looking at the native ligand on the ST2 protein receptor in the RCSB Database as a control. The native ligand for the ST2 Receptor is NAG [2-acetamido-2-deoxy-beta-D-glucopyranose] [32]. Using PubChem and drug bank, the molecular structure of the similarity with the native ligand is seen [33]. Drug candidate database was also collected using ChemBL with the keyword "ST2 inhibitor" [34]. After that, structural analysis was carried out using pharmacophore and obtained pharmacophore fit value. Then the 12 compounds in the docking process [35].

Docking process using PyRx

Docking of native ligands is carried out to find the 3D conformation of the native ligand to the Receptor by taking into account the coordinates of the center of mass of the structure and the grid box size of the binding site pocket angstroms [Vina] or several points [AutoDock]. The confirmation of the docking results obtained is aligned with the confirmation of the native ligand from the crystallographic measurements expressed in the root mean square deviation [RMSD] value [36]. The results of previous studies, the RMSD value for acceptable structural conformational alignment is less than 5; the closer the value to 0 is, the better the alignment value.

The AutoDock Vina tool, written in PyRx, was used to perform structure-based virtual screening utilizing docking simulations. Finally, the docked postures with FGFR Inhibitor were visually evaluated using PyMOL Molecular Graphics System.

RESULTS AND DISCUSSION

Cytoscape network electronic cigarette smokes

The results of the analysis of the content of e-Cigarette smokes are Nicotine, propylene glycol, glycerol, several Polycyclic Aromatic Hydrocarbons, carbonyl, and metals.

Predictions of e-Cigarette smoke targets on the body were collected from the Swiss Target Prediction database [http://www.swisstargetprediction.ch/] by inputting each molecular structure of the e-cigarette smoke in SDF format. The target protein data is then supplemented with UniProt ID data to uniform protein identity. Then the target protein data for the compounds contained in electronic cigarettes was then compiled in excel format and analyzed using Cytoscape. The higher the degree value indicates, the greater the significance of a node in the network. The greater the protein significance in cigarette smoke exposure at this stage, as shown in table 1.

Table 1: e-Cigarette smoke-related protein analyses using cytoscape 3.9.0

Gene name	Uniprot ID	Degree	Gene name	Uniprot ID	Degree
ALB	P02768	135	SLC6A4	P31645	42
STAT3	P40763	97	MMP2	P08253	42
HSP90AA1	P07900	97	PGR	P06401	42
CASP3	P42574	97	MAPK8	P45983	40
MAPK3	P27361	86	GSK3B	P49841	39
PTGS2	P35354	77	ACE	P12821	39
TLR4	O00206	68	HMOX1	P09601	39
MMP9	P14780	67	CDK2	P24941	38
EP300	Q09472	66	MPO	P05164	38
MAPK1	P28482	59	CASP9	P55211	38
NOS3	P29474	56	ABCB1	P08183	38
CCL2	P13500	55	TNFRSF1A	P19438	38
JAK2	O60674	55	PARP1	P09874	37
MAPK14	Q16539	55	MAOB	P27338	37
RELA	Q04206	54	MAOA	P21397	36
COMT	P21964	53	XIAP	P98170	36
PTPRC	P08575	51	DRD2	P14416	36
CXCR4	P61073	48	CDK1	P06493	36
KDR	P35968	46	SLC6A3	Q01959	35
VCAM1	P19320	45	ENSP00000459962	Q8NER1	35
HDAC1	Q13547	44	ACHE	P22303	35
MCL1	Q07820	43	GRM5	P41594	34
PIK3CA	P42336	43	CHRNA4	P43681	34
CNR1	P21554	43	NOS2	P35228	33
			CYP1A1	P04798	33

Using Cytoscape 3.9.0., we search protein-related e-cigarette smoke using the keyword e-Cigarette smoke on the STRING-Pubmed query. In the Cytoscape analysis, by identifying 366 nodes and 3256 edges [fig. above]. The top 49 proteins were selected, namely ALB, HSP90AA1, CASP3, STAT3, and so on, as shown in table 1. The higher the degree value indicates, the greater the significance of a node in the network, or at this stage, the greater the protein significance on exposure to electronic cigarettes.

COPD related targets in humans

STRING-diseases databases on Cytoscape can be used to create COPD target protein networks. By using the keyword "chronic obstructive pulmonary disease," we identified.

The data were then analyzed using Cytoscape software to identify proteins that have a significant role in the pathogenesis of COPD. Protein significance ratings for COPD pathogenesis are also used in

the COPD network, measured based on the degree value. The higher the degree value indicates, the greater the significance of a node in the network, or at this stage, it means the greater the protein significance in COPD pathogenesis.

Table 2 showed a COPD-related protein network; we evaluated and identified 1285 nodes and 32649 edges using Cytoscape analysis. The top 49 were selected, namely Tumor necrosis factor [TNF], interleukin 6 [IL6], and so on, as shown in table 2.

Cytoscape is a free, open-source software project that combines biomolecular interaction networks, high-throughput expression data, and other molecular states into a single conceptual framework. Although Cytoscape can be applied to any system with molecular components and interactions, it is most effective when combined with vast databases of protein-protein, protein-DNA, and genetic interactions, which are becoming more widely available for humans and models organisms [37].

Table 2: COPD-related protein analyses using cytoscape 3.9.0

Gene name	Uniprot ID	Degree	Gene name	Uniprot ID	Degree
TNF	P01375	510	IL4	P05112	270
IL6	P05231	499	ITGAM	P11215	267
AKT1	P31749	480	HIF1A	Q16665	254
ACTB	P60709	467	IL2	P60568	248
IL1B	P01584	444	ICAM1	P05362	244
ALB	Q8IUUK7	432	TLR2	O60603	243
TP53	Q8J016	390	CSF2	P04141	242
VEGFA	Q9H1W9	363	PPARG	Q15180	234
STAT3	P40763	359	PTEN	P60484	233
EGFR	Q9H2C9	352	IFNG	P01579	233
IL10	P22301	342	IL17A	Q16552	231
CXCL8	Q9UCS0	340	NOTCH1	P46531	229
FN1	H0Y4K8	325	IGF1	P05019	227
TLR4	Q5VZI9	321	STAT1	P42224	224
CTNNA1	P35222	321	PTGS2	P35354	223
MYC	P01106	320	FGF2	Q9UCS5	218
JUN	P05412	315	FOS	P01100	212
SRC	P12931	311	IL13	P24385	211
MAPK3	P27361	306	CCND1	P35225	211
CCL2	P13500	295	KRAS	P13501	202
MMP9	P14780	290	CCL5	P01116	202
EGF	P01133	286	CTLA4	Q96P43	201
CASP3	P42574	285	IL18	Q14116	196
PTPRC	P08575	276	HSPA4	P34932	195
CD8A	P01732	275			

Table 3: COPD-related protein network induced by the e-Cigarettes smokes analyses using cytoscape 3.9.0

Gene name	Uniprot ID	Degree	Gene name	Uniprot ID	Degree
ALB	Q8IUUK7	67	MAPK1	P28482	28
STAT3	P40763	51	MPO	P05164	28
CASP3	P42574	51	TNFRSF1A	P19438	27
TLR4	Q5VZI9	48	MMP2	P08253	27
MAPK3	P27361	45	KDR	P35968	25
PTGS2	P35354	45	MAPK8	P45983	24
MMP9	P14780	41	ACE	P12821	23
CCL2	P13500	36	MMP3	P08254	22
PTPRC	P08575	34	TLR9	Q9NR96	21
MAPK14	Q16539	30	JAK1	P23458	21
RELA	Q04206	30	GSK3B	P49841	21
HMOX1	P09601	29	PIK3CA	P42336	21
NOS3	Q548C1	29			

Identification of key receptors in the pathogenesis of COPD targeted by compounds contained in e-cigarettes smokes

This step is done by merging between two networks, namely the COPD-related protein network and the e-Cigarette smoke-related protein network. All target proteins that have a significant role in the pathogenesis of COPD exposed by e-cigarette smokers are identified from the combination of this network, as shown in table 3.

The Cytoscape analysis identified 114 nodes and 811 edges, and the receptors [proteins, genes, enzymes] were selected, namely ALB, STAT3, CASP3, and so on, as shown in table 3. The higher the degree value indicates, the greater the significance of a node in the network, or this stage, the greater the protein significance in the network. The pathogenesis of COPD exposed to cigarette smoke.

STAT3 is a signal transducer and transcriptional activator 3 that mediates cellular responses to interleukins, KITLG/SCF, LEP, and

other growth factors. STAT 3 binds to the interleukin-6 [IL-6] responsive element identified in the promoter of various acute-phase protein genes. STAT 3 is also activated by IL31 via IL31RA. Acts as a regulator of the inflammatory response by regulating the differentiation of naive CD4⁺ T cells into Th17 T-helper or regulatory T cells [Treg].

Then, a cytocluster was performed using Cytoscape for cluster analysis and visualization of the network using the website string and interactome for taking the highest degree of protein.

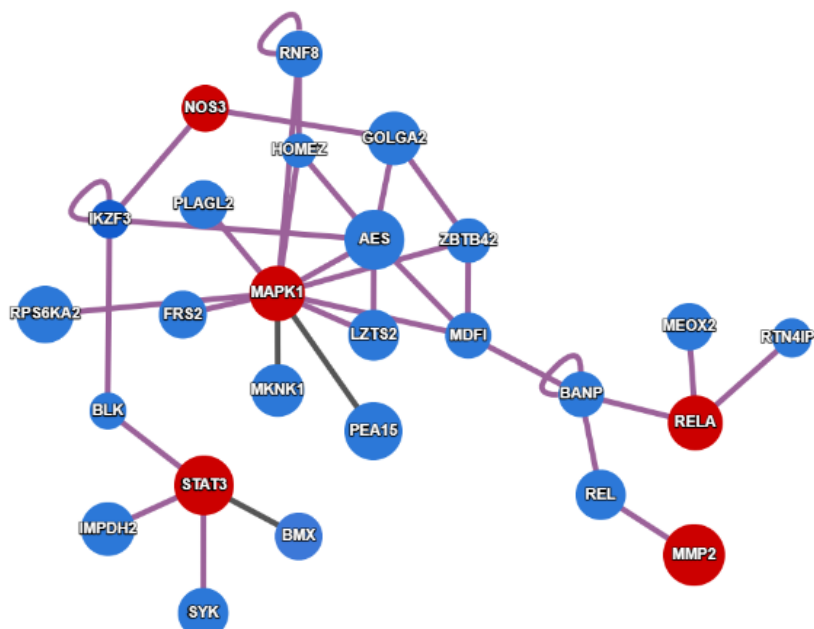


Fig. 1: COPD-related protein network induced by the e-cigarettes smoke

Table 4: Genes that play a role in COPD caused by exposure to e-cigarette smoke are analyzed by interactome

No	Gene name	Uniprot ID	Degree
1	STAT3	P40763-1	51
2	RELA	A0A087WVPO	30
3	NOS3	P29474	29
4	MAPK1	P28482-1	28
5	MMP2	P08253-1	27

Based on the network pharmacology analysis, 5 genes in COPD are caused by exposure to cigarette smoke, namely STAT3, RELA, NOS3, MAPK1, MMP2. Based on previous studies regarding these genes, they are activated after IL33 is bound to ST2.

Interleukin-33 [IL-33] is a non-hematopoietic cytokine primarily expressed in endothelial cells, epithelial cells, fibroblast-like cells, and myofibroblasts during homeostasis and in reaction to inflammation [38]. On target cells, IL-33 works by attaching to a heterodimeric receptor. Consisting of tumor suppressor tumorigenicity 2 [ST2, also known as IL-1RL1] and its co-receptor, the IL-1 receptor accessory protein [IL-1RAcP]. The presence of the ST2/IL-1RAcP binding process by IL-33 will activate the intracellular signaling pathway, which is mediated by the interaction of homotypic proteins with the MyD88 adapter molecule which then the next process occurs recruitment of IRAK and TRAF6, which leads to the expression of several inflammatory mediators through the activation of factors. nuclear-kB [NF-kB] and mitogen-activated protein kinase [MAPK] pathways. IL-33 activates various ST2-expressing tissue immune cells, ILC2s, mast cells, Th2 cells, regulatory T cells [Tregs], natural killer [NK] cells, eosinophils, basophils, dendritic cells, and alternatively activated macrophages are all examples of innate lymphoid cells [39].

Based on the analysis using interactome on the network pharmacology and its visualization in lung tissue, the protein with a red circle indicates that the protein has a high specificity and significant expression in lung tissue is STAT3, MAPK1, MMP2, RELA, NOS3.

This is in line with several steps previously carried out in the Cytoscape, where STAT3 ranks in the top 5 proteins with a higher value than other proteins. Then, when proceeded to analyze and visualize by interactomes, STAT3 still consistently affects the signaling, as seen from the picture above.

The reaction induced by the binding of IL-33 with ST2, which will activate STAT3 in the cytoplasm, will then translocate in the nucleus previously in the upstream pathway mediated by the JAK2 signaling pathway. Then, on the other hand, the RELA gene will be activated after binding IL-33 with ST2 mediated by the MAPK signaling pathway and NF-kB. At the same time, the MAPK1 gene will be activated after binding of IL-33 with ST2 mediated by the MAP3K8 signaling pathway by phosphorylation to produce MAP2K1 and MAP2K2. All these processes are depicted by dotted arrows, which indicate that the reactions through these mechanisms are currently not known with certainty [39].

Selection of candidate drug based on pharmacophore mapping

ST2 receptor validation

ST2 Receptor/Interleukin-1 receptor-like 1 [IL1RL1] for docking step was obtained from the RCSB database with the keywords "ST2" or with the synonym "IL1RL1". ST2 Receptor/Interleukin-1 receptor-like 1 on RCSB obtained 3 proteins with RCSB ID: 4KC3, 1IRA, and IG0Y. To find out whether these proteins can be used in the docking process, evaluation was carried out in 3 ways. Firstly by analyzing the data on the RCSB database, such as the resolution condition where a good resolution is less than 3Å, wwPDB

Validation percentile ranks, and ligand structure quality assessment. The second evaluation method is to access PDBSUM using the Ramachandran plot and evaluate the most favored value of at least 90% and the G factor. The third method is analyzing a missing residue by PyMol.

4KC3

4KC3 is a cytokine/receptor binary complex with a resolution of 3.27Å, and the structural validation of 4KC3 is not good. Evaluation of wwPDB validation percentile ranks showed the data is more towards red, not blue, as shown in fig. 2.

Deposited: 2013-04-24 Released: 2013-08-28
Deposition Author(s): Liu, X., Wang, X.Q.

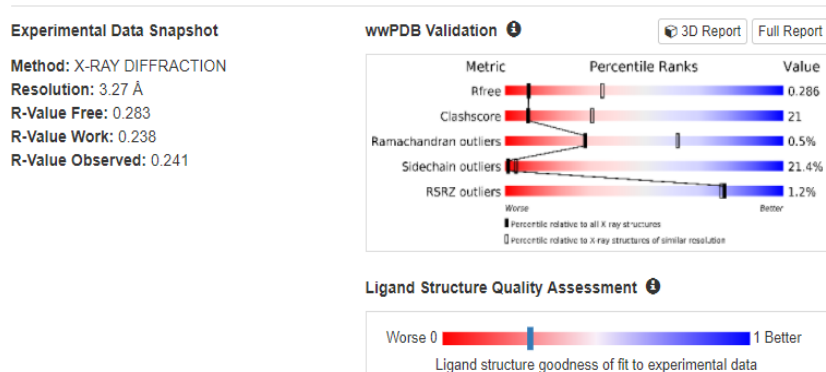


Fig. 2: RCSB data for 4KC3

In the Ramachandran plot analysis, as shown in fig. 3, a good structure's most favored structure is at least 90%, while in 4KC3, the most favored value is 86.1%. This data indicated that the structure

of 4KC3 is not good. Similarly, the G factor analysis results resulted in -0.30, categorized as highly unusual, and showed a less good structure, as shown in fig. 3.

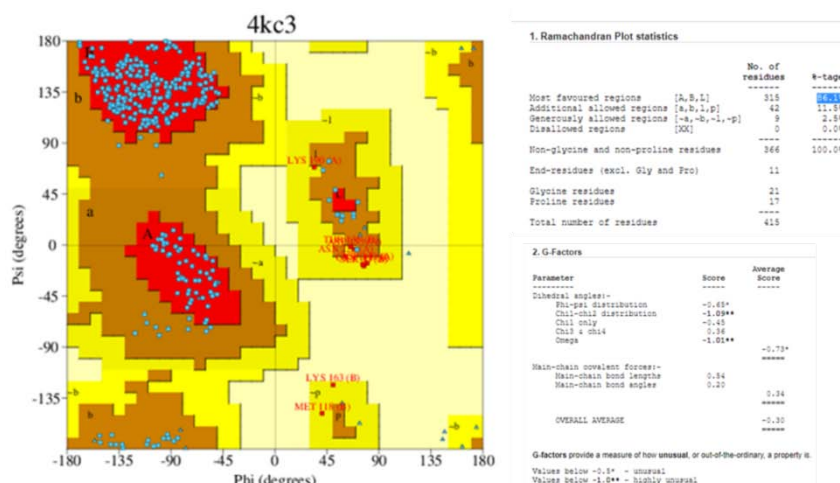


Fig. 3: Ramachandran plot analysis of 4KC3

Deposited: 1998-04-09 Released: 1998-06-17

Deposition Author(s): Schreuder, H.A., Tardif, C., Tramp-Kalmeyer, S., Soffientini, A., Sarubbi, E., Akeson, A., Bowlin, T., Yanofsky, S., Barrett, R.W.

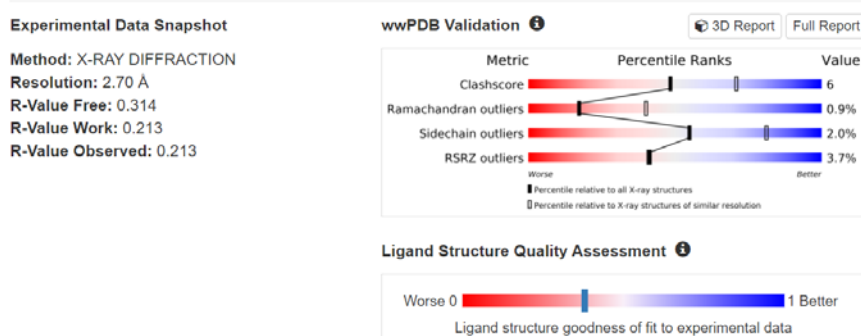


Fig. 4: RCSB data for 1IRA

1IRA

1IRA is an interleukin-1 receptor complex with an interleukin-1 receptor antagonist [IL1RA] with a resolution of 2.70 Å, and the structural validation is categorized as quite good compared to 4KC3. Evaluation of wwPDB validation percentile ranks showed red and blue colors, as shown in fig. 4.

In the analysis using the Ramachandran plot as shown in fig. 5, a good structure's most favored structure is at least 90%, while in 1IRA, the most favored value is 86.7%, categorized as not good structure. Similarly, the G factor analysis results resulted in 0.26, categorized as highly unusual, and showed good structure, as shown in fig. 5.

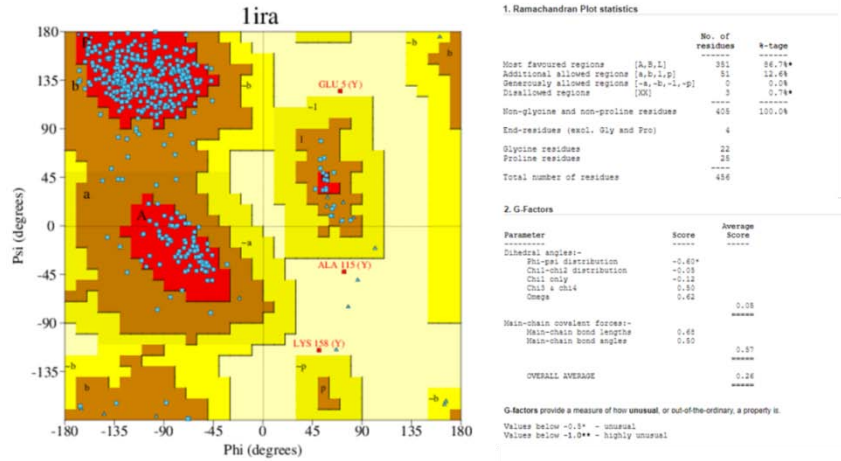


Fig. 5: Ramachandran plot analysis of 1IRA

Deposited: 2000-10-09 Released: 2000-10-25

Deposition Author(s): Vigers, G.P.A., Dripps, D.J., Edwards, C.K., Brandhuber, B.J.

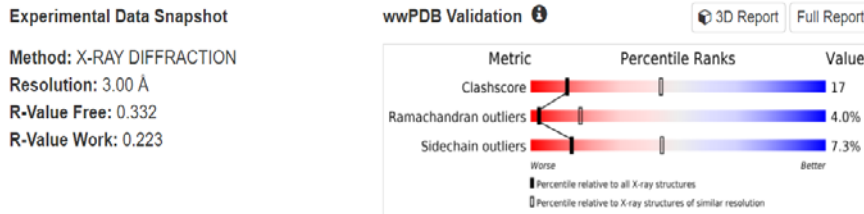


Fig. 6: RCSB data for 1G0Y

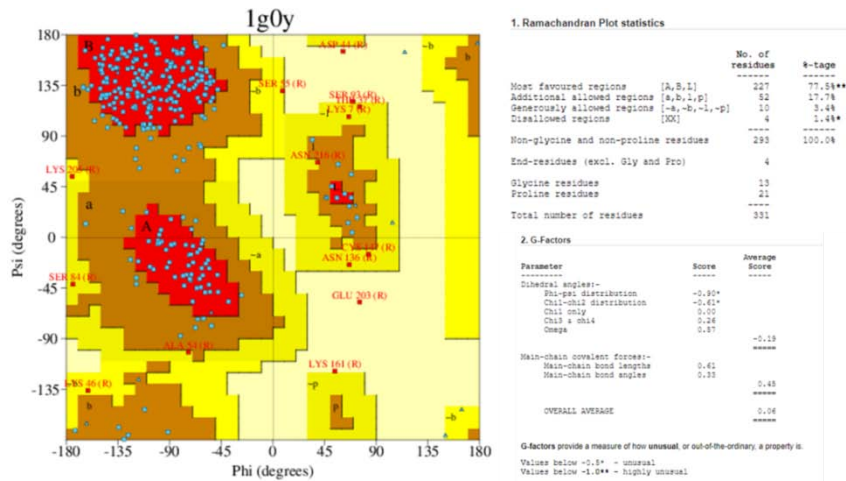


Fig. 7: Ramachandran plot analysis of 1G0Y

Based on the validation results of the protein receptor for ST2, a protein is used as a receptor with PDB ID: 1IRA. Because it has a better evaluation result compared to 4KC3 and IG0Y according to a resolution of 2.70 Å, wwPDB Validation percentile ranks and ligand structure quality assessment, and the results PDBSUM uses the Ramachandran plot and shows the most favored value, which is better compared to other proteins, and after analyzed by PyMol software, a protein with PDB ID 1IRA it has no missing residue in its sequence. Then the PDB format is downloaded, and the receptor preparation is carried out using a CHIMERA.

Analysis of ligands and drug candidates from the database in pubchem

The discovery of drug candidates begins with analyzing the native ligand as a control on the ST2 protein receptor in the RCSB database[40], namely the NAG ligand [2-acetamido-2-deoxy-beta-D-glucopyranose]. Then, the structural similarity with the native ligand was analyzed using PubChem and drug bank. Database collection was also carried out on them with the keyword "ST2 inhibitor". Then after that, a structure-based analysis was performed using pharmacophore and obtained pharmacophore fit values and 12 drug candidates. Then the 12 drug candidates were docked using PyRx.

In the analysis of NAG ligands with three chains, namely C, D, E, it can be concluded that in its structure, there are active sites in the group, namely hydrogen bond acceptors 5 and hydrogen bond donors 4, where the red color represents a hydrogen bond acceptor. In contrast, the green color represents a hydrogen bond donor. Hydrogen bond donors.

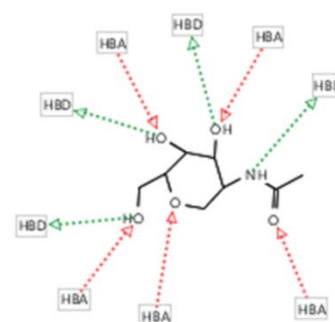


Fig. 8: Structure of NAG, the native ST2 ligand analyzed by Ligandscout 4.4.7

Table 5: Drug candidates were analyzed by the structural similarity with the native ligand using PubChem and drug bank

Compound name	PUBCHEM ID
N acetylmannosamine	11096158
Aceneuramic acid	14017587
Ceramide AP/N-[2-Hydroxyoctadecanoyl]-hydroxysphinganine	44625889
Ceramide NP/N-oleoylphytyosphingosine	57378373
Hg9a-9, Nonanoyl-N-hydroxyethylglucamide	46936271
N-Acetyl-2-deoxy-2-amino-galactose	84265
N-Acetylactosamine	9800166
MLi/2,6-dimethyl-4-[6-[5-[1-methylcyclopropyl] oxy-1H-indazol-3-yl] pyrimidin-4-yl] morpholine	78319901
Terazosin	5401
BMS-911543	50922691
NAG Inhibitor	657356
FGFR Inhibitor/Debio-1347/sodium; 2-amino-5-[1-methoxy-2-methylindolizine-3-carbonyl] benzoate	68853159

Data on the physicochemical properties of the candidate drug based on Lipinski's rule of five

Condition:

1. BM<500 mg/mol
2. Log P<5
3. Hydrogen Donor<5
4. Hydrogen Acceptor<10

Then, after all the ligands and receptors have been prepared using a CHIMERA, docking is done using PyRx, and then a visualization analysis is performed using Discovery Studio.

From the docking results, the smallest or more negative binding affinity values are obtained. The stronger the FGFR Inhibitor ligand showed the interaction with the Receptor with a binding affinity value of -9.0 kcal/mol with mode/position 0, and RMSD 0.0. The second smallest binding affinity value is the NAG ligand with a -8.5 kcal/mol with mode/position 0 and RMSD 0.0.

Table 6: Virtual docking result using PyRx

Ligand	Binding affinity (kcal/mol)	Mode	RMSD lower bound	Rmsd upper bound
lira_sudah_pymol_FGFR_sudah_chim	-9.0	0	0.0	0.0
lira_sudah_pymol_FGFR_sudah_chim	-8.7	1	2.613	-4.877
lira_sudah_pymol_DAG_sudah_chim	-8.5	0	0.0	0.0
lira_sudah_pymol_FGFR_sudah_chim	-8.5	2	1.308	2.153
lira_sudah_pymol_FGFR_sudah_chim	-8.4	3	2.662	4.972
lira_sudah_pymol_FGFR_sudah_chim	-8.4	4	34.334	35.803
lira_sudah_pymol_DAG_sudah_chim	-8.3	1	4.113	6.771
lira_sudah_pymol_DAG_sudah_chim	-8.2	2	42.947	44.754
lira_sudah_pymol_FGFR_sudah_chim	-8.2	5	33.673	35.101
lira_sudah_pymol_FGFR_sudah_chim	-8.2	6	45.012	47.238
lira_sudah_pymol_DAG_sudah_chim	-8.1	3	42.569	45.078
lira_sudah_pymol_FGFR_sudah_chim	-8.1	7	47.032	49.28
lira_sudah_pymol_DAG_sudah_chim	-8.0	4	43.847	46.753
lira_sudah_pymol_DAG_sudah_chim	-7.9	5	42.803	45.273
lira_sudah_pymol_DAG_sudah_chim	-7.9	6	41.674	44.734
lira_sudah_pymol_FGFR_sudah_chim	-7.9	8	45.612	47.83
lira_sudah_pymol_DAG_sudah_chim	-7.7	7	31.699	35.315
lira_sudah_pymol_DAG_sudah_chim	-7.7	8	42.306	44.532
lira_sudah_pymol_MLi_sudah_chim	-7.5	0	0.0	0.0
lira_sudah_pymol_HG9a_sudah_chim	-7.0	0	0.0	0.0
lira_sudah_pymol_MLi_sudah_chim	-7.0	1	49.437	51.73
lira_sudah_pymol_MLi_sudah_chim	-6.9	2	17.969	19.942

Then using PyMol, the FGFR and NAG ligands from the docking results were visualized together with their receptors to visualize the location of their binding.

The following results were obtained: green is the NAG ligand, while blue is the FGFR Inhibitor ligand.

Then after knowing the binding position of the ligand to its Receptor, further visualization was carried out using the Discovery Studio to determine the interaction of amino acids in the binding.

The results of the interaction of amino acids on the NAG ligand are shown in the image below:

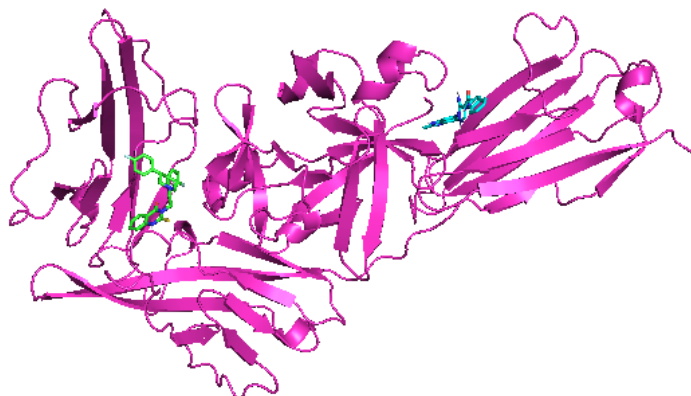


Fig. 9: Visualization of the binding of ST2 Receptor with native ligand NAG and FGFR inhibitor ligand. The purple is the ST2 Receptor, the green is the NAG ligand, and the blue is the FGFR Inhibitor ligand

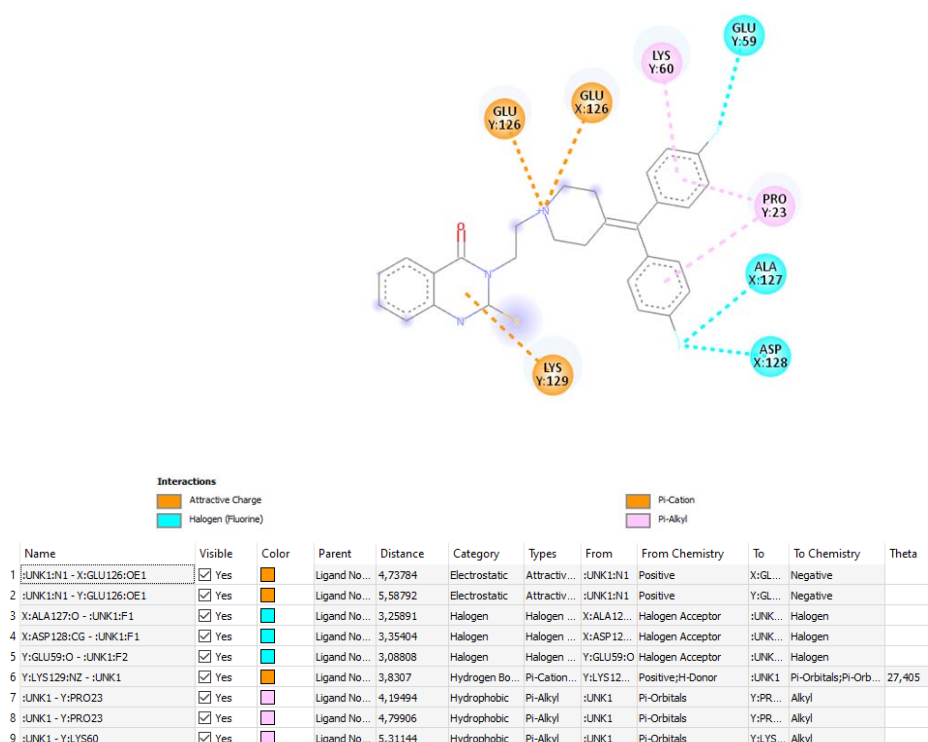


Fig. 10: The interaction of amino acids of the ST2 receptor on the NAG as a native ligand

The NAG ligand interacts with the amino acid glutamate at the number 126 chain X with an electrostatic interaction type with a bond distance of 4.73 Å. The NAG ligand interacts with the glu amino acid at the number 126 chain Y with an electrostatic interaction type with a bond distance of 5.58 Å. The NAG ligand interacts with the amino acid alanine on the number 127 chain X with a halogen bond interaction type with a bond distance of 3.25 Å. The NAG ligand interacts with the amino acid aspartate at number 128 chain X with the type of interaction of the halogen bond with a bond distance of 3.35 Å. The NAG ligand interacts with the amino acid glutamate at

the number 59 chain Y with a halogen bond interaction type with a bond distance of 3.08 Å. The NAG ligand interacts with the amino acid lysine at the number 129 chain Y with a hydrogen bond interaction type with a bond distance of 3.83 Å.

The NAG ligand interacts with the proline amino acid at number 23 chain Y with a hydrophobic bond interaction type with a bond distance of 4.19 Å and 4.7 Å. The NAG ligand interacts with the amino acid lysine at number 60 chain Y with a hydrophobic interaction type with a bond distance of 5.31 Å.

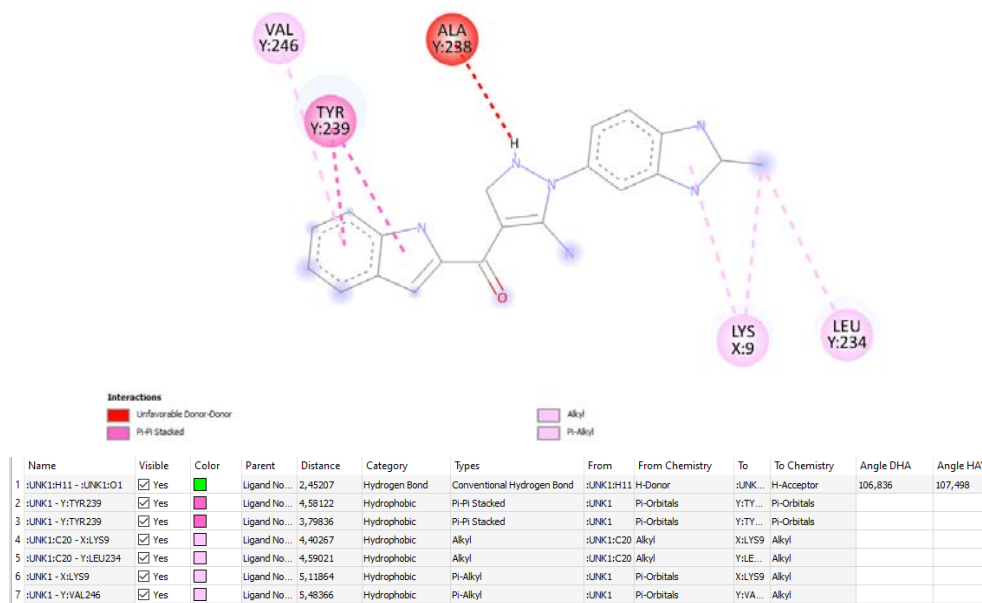


Fig. 11: The interaction of amino acids of the ST2 Receptor on the FGFR inhibitor as a ligand

The FGFR ligand interacts with hydrogen and oxygen atoms by hydrogen bonding interaction with a bond distance of 2.45 Å. The FGFR ligand interacts with the amino acid tyrosine at number 236 chain Y with a hydrophobic interaction type with a bond distance of 4.58 Å. The FGFR ligand interacts with the amino acid tyrosine on the number 239 chain Y with a hydrophobic interaction type with a bond distance of 3.79 Å. The FGFR ligand interacts with the amino acid lysine at number 9 chain X with a hydrophobic bond interaction type with a bond distance of 4.40 Å. The FGFR ligand interacts with the amino acid leucine at number 234 chain Y with a hydrophobic bond interaction type with a bond distance of 4.59 Å. The FGFR ligand interacts with the amino acid lysine at number 9 chain X with a hydrophobic bond interaction type with a bond distance of 5.11 Å. The FGFR ligand interacts with the amino acid valine at number 246 chain Y with a hydrophobic bond interaction type with a bond distance of 5.48 Å.

CONCLUSION

Our research provides functional evidence to reveal the prediction of their potential targets and FGFR Inhibitor mechanism pathways. The findings revealed that FGFR Inhibitor was a suitable repurposing medication for anti-COPD development via the IL-33/ST-2 signaling pathway.

To verify this *in silico* study, more research on the IL-33/ST-2 signaling inhibitor of FGFR Inhibitor and the underlying mechanism is needed in other approaches such as *in vitro*, *in vivo*, and clinical study evaluation.

DATA AVAILABILITY

The data supporting this study's findings are available from the corresponding author, [AB], upon reasonable request.

ACKNOWLEDGMENT

This research was supported by The Ministry of Research and Technology/BRIN Republic of Indonesia 2021. NKB 058/UN2. RST/HKP.05.00/2021

FUNDING

Nil

AUTHORS CONTRIBUTIONS

All the authors have contributed equally.

CONFLICTS OF INTERESTS

There are no conflicts of interest.

REFERENCES

1. Twyman L, Watts C, Chapman K, Walsberger SC. Electronic cigarette use in New South Wales, Australia: reasons for use, place of purchase and use in enclosed and outdoor places. *Aust N Z J Public Health*. 2018 Oct 1;42(5):491-6. doi: 10.1111/1753-6405.12822, PMID 30152006.
2. Bozier J, Chivers EK, Chapman DG, Larcombe AN, Bastian NA, Masso Silva JA, Byun MK, McDonald CF, Crotty Alexander LE, Ween MP. The evolving landscape of e-cigarettes: A systematic review of recent evidence. *Chest*. 2020 May 1;157(5):1362-90. doi: 10.1016/j.chest.2019.12.042. PMID 32006591.
3. Ghosh A, Coakley RC, Mascenik T, Rowell TR, Davis ES, Rogers K. Chronic E-cigarette exposure alters the human bronchial epithelial proteome. *Am J Respir Crit Care Med*. 2018 Jul 1;198(1):67-76. doi: 10.1164/rccm.201710-20330C, PMID 29481290.
4. Fischer BM, Pavlisko E, Voynow JA. Pathogenic triad in COPD: oxidative stress, protease-antiprotease imbalance, and inflammation. *Int J Chron Obstruct Pulm Dis*. 2011;6:413-21. doi: 10.2147/COPD.S10770, PMID 21857781.
5. Nugroho Eko Wd, Lestari Dwii Nmb. The role of pulmonary rehabilitation in acute exacerbations of chronic obstructive pulmonary disease. *Rahmad, Narasati S. Int J Appl Pharm*. 2020 Oct 15;12:39-40.
6. Herr C, Han G, Li D, Tschernig T, Dinh QT, Beißwenger C. Combined exposure to bacteria and cigarette smoke resembles characteristic phenotypes of human COPD in a murine disease model. *Exp Toxicol Pathol*. 2015;67(3):261-9. doi: 10.1016/j.etp.2015.01.002, PMID 25601416.
7. Chen J, Zhou H, Wang J, Zhang B, Liu F, Huang J. Therapeutic effects of resveratrol in a mouse model of HDM-induced allergic asthma. *Int Immunopharmacol*. 2015;25(1):43-8. doi: 10.1016/j.intimp.2015.01.013, PMID 25617148.
8. Milevoj Kopcinovic L, Domijan AM, Posavac K, Cepelak I, Zanic Grubisic T, Rumora L. Systemic redox imbalance in stable chronic obstructive pulmonary disease. *Biomarkers*. 2016 Nov 16;21(8):692-8. doi: 10.3109/1354750X.2016.1172110, PMID 27121533.
9. Barnes PJ. Inhaled corticosteroids in COPD: A controversy. *Respiration*. 2010;80(2):89-95. doi: 10.1159/000315416, PMID 20501985.
10. Boardman C, Chachi L, Gavril A, Keenan CR, Perry MM, Xia YC. Mechanisms of glucocorticoid action and insensitivity in airways disease. *Pulm Pharmacol Ther*. 2014;29(2):129-43. doi: 10.1016/j.pupt.2014.08.008, PMID 25218650.

11. Barnes PJ. Cellular and molecular mechanisms of asthma and COPD. *Clin Sci (Lond)*. 2017;131(13):1541-58. doi: 10.1042/CS20160487, PMID 28659395.
12. Chong J, Leung B, Poole P. Phosphodiesterase 4 inhibitors for chronic obstructive pulmonary disease. *Cochrane Database Syst Rev*. 2017 Sep 19;9(9):CD002309-CD002309. doi: 10.1002/14651858.CD002309.pub5.
13. Kawamatawong T. Roles of roflumilast, a selective phosphodiesterase 4 inhibitor, in airway diseases. *J Thorac Dis*. 2017 Apr;9(4):1144-54. doi: 10.21037/jtd.2017.03.116, PMID 28523172.
14. Khan PA, Sujala A, Nousheen BbS, Fatima AF, Ala HT, Reddy Abt P. A comparative evaluation of the efficacy of triple-drug therapy with dual drug therapy in COPD patients. *Int J Pharm Pharm Sci*. 2018 Apr 1;10(4):105-9. doi: 10.22159/ijpps.2018v10i4.24529.
15. Unni A, Jayaprakash AK, McY P, Drug UD. Utilization pattern in chronic obstructive pulmonary disease inpatients at a tertiary care Hospital. *Int J Pharm Pharm Sci*. 2015 Nov 1;7(11):389-91.
16. Wang C, Zhou J, Wang J, Li S, Fukunaga A, Yodoi J, Tian H. Progress in the mechanism and targeted drug therapy for COPD. *Signal Transduct Target Ther*. 2020;5(1):248. doi: 10.1038/s41392-020-00345-x, PMID 33110061.
17. Lingel A, Weiss TM, Niebuhr M, Pan B, Appleton BA, Wiesmann C. Structure of IL-33 and its interaction with the ST2 and IL-1RAcP receptors-insight into heterotrimeric IL-1 signaling complexes. *Structure*. 2009;17(10):1398-410. doi: 10.1016/j.str.2009.08.009, PMID 19836339.
18. Qiu C, Li Y, Li M, Li M, Liu X, McSharry C. Anti-interleukin-33 inhibits cigarette smoke-induced lung inflammation in mice. *Immunology*. 2013 Jan;138(1):76-82. doi: 10.1111/imm.12020, PMID 23078031.
19. Cunningham A, McAdam K, Thissen J, Digard H. The evolving E-cigarette: comparative chemical analyses of E-cigarette vapor and cigarette smoke. *Front Toxicol*. 2020;2:7. doi: 10.3389/ftox.2020.586674.
20. Gfeller D, Grosdidier A, Wirth M, Daina, Michielin O, Zoete V. Swiss target prediction: A web server for target prediction of bioactive small molecules. *Nucleic Acids Res*. 2014;42(W1):W32-8. doi: 10.1093/nar/gku293.
21. Han L, Wang Y, Bryant SH. A survey of across-target bioactivity results of small molecules in PubChem. *Bioinformatics*. 2009 Sep 1;25(17):2251-5. doi: 10.1093/bioinformatics/btp380, PMID 19549631.
22. Safran M, Dalah I, Alexander J, Rosen N, Iny Stein T, Shmoish M, Nativ N, Bahir I, Doniger T, Krug H, Sirota Madi A, Olender T, Golan Y, Stelzer G, Harel A, Lancet D. GeneCards version 3: the human gene integrator. *Database (Oxford)* Version 3. 2010 Jan 1;2010:baq020. doi: 10.1093/database/baq020, PMID 20689021.
23. Amberger JS, Bocchini CA, Schiettecatte F, Scott AF, Hamosh A. Online mendelian inheritance in man (OMIM®), an online catalog of human genes and genetic disorders. *Nucleic Acids Res*. 2015 Jan 28;43:D789-98. doi: 10.1093/nar/gku1205, PMID 25428349.
24. Wu L, Chen Y, Yi J, Zhuang Y, Cui L, Ye C. Mechanism of action of Bu-Fei-Yi-Shen formula in treating chronic obstructive pulmonary disease based on network pharmacology analysis and molecular docking validation. *BioMed Res Int*. 2020;2020:9105972. doi: 10.1155/2020/9105972.
25. Tang Y, Li M, Wang J, Pan Y, Wu FX. CytoNCA: a cytoscape plugin for centrality analysis and evaluation of protein interaction networks. *Biosystems*. 2015;127:67-72. doi: 10.1016/j.biosystems.2014.11.005. PMID 25451770.
26. Rao VS, Srinivas K, Sujini GN, Kumar GNS. Protein-protein interaction detection: methods and analysis. *Int J Proteomics*. 2014;2014:147648. doi: 10.1155/2014/147648.
27. Zhang Y, Gao P, Yuan JS. Plant protein-protein interaction network and interactome. *Curr Genomics*. 2010 Mar;11(1):40-6. doi: 10.2174/138920210790218016, PMID 20808522.
28. Gore S, Sanz Garcia E, Hendrickx PMS, Gutmanas A, Westbrook JD, Yang H. Validation of structures in the protein data bank. *Structure*. 2017;25(12):1916-27. doi: 10.1016/j.str.2017.10.009, PMID 29174494.
29. Majorek KA, Zimmerman MD, Grabowski M, Shabalin IG, Zheng H, Minor W. Assessment of crystallographic structure quality and protein-ligand complex structure validation. *Wiley Online Books*. 2020. p. 253-75. doi: 10.1002/9781118681121.
30. Laskowski RA, Jablonska J, Pravda L, Varekova RS, Thornton JM. PDBsum: structural summaries of PDB entries. *Protein Sci*. 2018 Jan 1;27(1):129-34. doi: 10.1002/pro.3289, PMID 28875543.
31. Sladek V, Yamamoto Y, Harada R, Shoji M, Shigeta Y, Sladek V. pyProGA-A PyMOL plugin for protein residue network analysis. *Plos One*. 2021 Jul 30;16(7):e0255167. doi: 10.1371/journal.pone.0255167. PMID 34329304.
32. Homsak E, Gruson D. Soluble ST2: A complex and diverse role in several diseases. *Clin Chim Acta*. 2020;507:75-87. doi: 10.1016/j.cca.2020.04.011, PMID 32305537.
33. Wishart DS, Knox C, Guo AC, Shrivastava S, Hassanali M, Stothard P. DrugBank: a comprehensive resource for in silico drug discovery and exploration. *Nucleic Acids Res*. 2006 Jan 1;34:D668-72. doi: 10.1093/nar/gkj067, PMID 16381955.
34. Buhlmann S, Reymond JL. ChEMBL-likeness score and database GDBChEMBL. *Front Chem*. 2020;8:46. doi: 10.3389/fchem.2020.00046, PMID 32117874.
35. Opo FADM, Rahman MM, Ahammad F, Ahmed I, Bhuiyan MA, Asiri AM. Structure-based pharmacophore modeling, virtual screening, molecular docking and ADMET approaches for identification of natural anti-cancer agents targeting XIAP protein. *Sci Rep*. 2021;11(1):40-9. doi: 10.1038/s41598-021-83626-x, PMID 33603068.
36. Sargis D, J OA. Small-molecule library screening by docking with PyRx. *J Chem Biol*. 2014;243-50.
37. Shannon P, Markiel A, Ozier O, Baliga NS, Wang JT, Ramage D. Cytoscape: a software environment for integrated models of biomolecular interaction networks. *Genome Res*. 2003 Nov;13(11):2498-504. doi: 10.1101/gr.1239303, PMID 14597658.
38. Kim RY, Oliver BG, Wark PAB, Hansbro PM, Donovan C. COPD exacerbations: targeting IL-33 as a new therapy. *Lancet Respir Med*. 2021 Oct 31;9(11):1213-4. doi: 10.1016/S2213-2600(21)00182-X, PMID 34302759.
39. Pinto SM, Subbannayya Y, Rex DAB, Raju R, Chatterjee O, Advani J. A network map of IL-33 signaling pathway. *J Cell Commun Signal*. 2018;12(3):615-24. doi: 10.1007/s12079-018-0464-4, PMID 29705949.
40. Berman HM. The protein data bank. *Nucleic Acids Res*. 2000 Jan 1;28(1):235-42. doi: 10.1093/nar/28.1.235.